RESEARCH ARTICLE

Land Use Change and Its Impact on Carbon Stock in Yellow River Basin from 2000 to 2020

Ma Yali[1*], Adam Aruldewan S.Muthuveeran[1], Mohd Johari Mohd Yusof[1], Gao Yuxuan[1], Liu Peng[2]

[1]Department of Landscape Architecture, Faculty of Design and Architecture, Universiti Putra Malaysia, Serdang Selangor
[2]Art and Media College, Chongqing Metropolitan College of Science and Technology, Yongchuan, Chongqing China

*Corresponding author: gs64967@student.upm.edu.my

Abstract

The Yellow River Basin serves as a crucial ecological corridor and carbon sink in China. Despite concerted efforts towards ecological restoration, the growth of carbon stocks had been hindered by the impacts of climate change and human activities. Land use change plays a critical role in modifying ecosystem structure and biogeochemical processes, thereby impacting carbon stock dynamics. This study utilized the InVEST model to analyze land use data from 2000, 2010, and 2020 to calculate changes in carbon stocks. The findings indicate that: (1) built-up land expanded substantially by 22,247 km² (+151.8%), while unused land declined sharply by 21,960 km² (−49.3%), whereas cropland, grassland, and forest remained relatively stable; (2) total carbon stocks increased by 110.9 × 10^6 t, but growth slowed markedly, with +89.5 × 10^6 t gained in 2000–2010 and only +21.4 × 10^6 t in 2010–2020; (3) Land-use transitions were the dominant drivers: grassland-to-forest conversion contributed +120.2 × 10^6 t, while forest-to-grassland conversion caused −140.2 × 10^6 t, and unused-to-built-up transitions resulted in −60.1 × 10^6 t loss. Integrating land use dynamics and transition matrices, the study clarifies land use evolution and carbon impacts, supporting regional land use optimization and Carbon Neutrality.

Keywords: *Yellow River Basin; Carbon Stock; Land Use; InVEST Model*

Citation:
Ma, Y., Muthuveeran, A. A. S., Mohd Yusof, M. J., Gao, Y., & Liu, P. (2025). Land use change and its impact on carbon stock in Yellow River Basin from 2000 to 2020. Alam Cipta, 18(Special Issue 2), [Article 12]. https://doi.org/10.47836/AC.18.S2.PAPER12

Received:
07 February 2025

Accepted:
14 October 2025

Published:
November 2025

Introduction

The carbon stock of terrestrial ecosystems serves as a fundamental component of the global carbon cycle and critically contributes to climate change mitigation. As a core indicator of ecosystem service functionality, carbon stock is highly sensitive to land use changes driven by multiple factors including urban expansion, agricultural intensification, and population growth. Land use not only reshapes land-use patterns but also disrupts ecological processes by altering soil and vegetation carbon densities, thereby impacting regional and global carbon dynamics (Huang & Wang, 2023).

The Yellow River Basin (YRB), stretching from the Qinghai-Tibet Plateau to the alluvial plains of eastern China, represents a crucial ecological and geographical region with significant implications for national environmental security. As a critical ecological barrier, the basin has undergone significant land use transformations over the past two decades due to escalating anthropogenic activities and large-scale ecological restoration initiatives such as the Grain for Green Program. These changes, in conjunction with urbanization intensification and land degradation, have raised urgent concerns regarding the region's capacity to sustain its carbon sink capacity and uphold essential ecosystem services. Therefore, it is imperative to comprehend the implications of land use change on carbon stock in this dynamic and ecologically sensitive region.

In recent years, driven by the goals of Carbon Neutrality and ecological civilization, the impact of land use change on ecosystem carbon stocks has become a research hotspot in geography, ecology, and environmental sciences. In the YRB, most studies have employed the InVEST model to estimate carbon stocks and analyze their spatial distribution patterns, yet their emphases differ. For example, Zeng et al. (2024) and Li et al. (2025) used MGWR and OPGD models, respectively, to explore the drivers of carbon stock, while Yang (2021) focused on future land-use conversions under policy scenarios. Li et al. (2025) also incorporated transition matrices and contribution rates to quantify the effects of land conversions, but their analysis did not fully capture the dynamic characteristics of land use changes and the specific pathways of transitions. Existing research has rarely applied land use dynamic indices and transition matrices in a systematic way to finely characterize the bidirectional conversions between land-use types, nor has it clearly identified which transitions serve as the major drivers of carbon stock changes in the YRB.

This study utilizes high-resolution land use datasets from 2000 to 2020 and employs the InVEST model to comprehensively analyze the spatiotemporal characteristics of land use change and its impacts on carbon stock in the Yellow River Basin. By integrating dynamic land use patterns with a transfer matrix, this study aims to elucidate the spatiotemporal evolution characteristics of land use in the Yellow River Basin from 2000 to 2020 and its impact on carbon stocks.

Study Area and Data Sources

Study Area

The YRB is situated in the north-central part of China (95°53′ E - 119°05′ E, 32°10′ N - 41°50′ N), spanning from the Bayan Har Mountains to the Bohai Sea, encompassing the Yinshan Mountains and the Qinling Mountains, with a total area of 795000 km^2 (Jian et al., 2022; Xu et al., 2023). The YRB exhibits a pronounced altitudinal gradient, with higher elevations in the western region and lower elevations in the eastern region. This encompasses four significant topographic gradients, namely the Tibetan Plateau, Inner Mongolia Plateau, Loess Plateau, North China Plain and Huanghuaihai Plain (Li et al., 2020; Sun et al., 2023; Wang et al., 2022). The western source region, characterized by towering mountain ranges, perpetual snow cover, and well-developed glacial landforms, exhibits an average elevation exceeding 4,000 meters. The central region, situated at elevations between 1,000 and 2,000 meters, is predominantly marked by expansive loess landforms that are highly susceptible to severe soil erosion. In contrast, the eastern region primarily comprises the Yellow River alluvial plain with elevations generally below 50 meters.

Data Sources

The vector boundary data for the YRB was sourced from the http://www.geodata.cn/ provided by Ma (2014). Land use data for the years 2000, 2010, and 2020 were derived from Globe Land 30 https://www.webmap.cn/commres.do?method=globeIndex provided by National Geomatics Center of China, with a spatial resolution of 30 m × 30 m. Following the primary classification standard for land use types, the data were reclassified into six distinct categories: water bodies, cropland, grassland, forest, built-up land, and unused land. Carbon density data corresponding to different land use categories were procured from 2010s China Terrestrial Ecosystem Carbon Density Dataset (Xu et al., 2019) and further informed by references to relevant academic literature (Xu et al., 2023). The calibration of carbon density utilized annual average temperature and precipitation datasets, which were retrieved from the National Earth System Science Data

Center provided by Peng et al. (2019) https://www.geodata.cn/data/datadetails.html?dataguid=164304785536614&docId=490. These datasets include the China 1 km resolution monthly precipitation dataset (1901–2023) and the 1 km resolution monthly average temperature dataset, providing high-resolution climatological data essential for refining carbon density estimations.

Methodology

Land Use Dynamics

The degree of land use dynamics can be categorized into two types: single land use dynamic degree and comprehensive land use dynamic degree. The proposed model enables a quantitative description of the dynamic changes in land use types, thereby accurately reflecting the rate and extent of changes in land use types within the study area (Chen et al., 2021; Zhang, 2022). The single land use dynamic degree refers to the rate of change for a specific land use category over a given period, whereas the comprehensive land use dynamic degree represents the overall extent of land use transitions across all categories within the same timeframe.

The formula for the single land use dynamic degree is as follows:

$$K = \frac{U_b - U_a}{U_a} \times \frac{1}{T} \times 100\% \quad (1)$$

K represents the single land-use dynamic degree index, while U_b and U_a denote the area of a specific land use category at the end and the beginning of the study period, respectively. T refers to the temporal scale of the study period. A positive K value indicates an expansion in the land use category during the study period. Conversely, a negative K value reflects a reduction in area. The magnitude of, regardless of its sign, signifies the intensity of change, with larger absolute values representing more pronounced transformations within the specified land use category.

The formula for the comprehensive land use dynamic degree is as follows:

$$LC = \frac{\sum_{i=1}^{n} \Delta LU_{i-j}}{2\sum_{i=1}^{n} \Delta LU_i} \times \frac{1}{T} \times 100\% \quad (2)$$

where LC represents the comprehensive land use dynamic degree index, LU_i denotes the quantity of the i-th land use type at the beginning of the study period, and ΔLU_{i-j} refers to the total quantity of the i-th land use type that transitioned to other land use types during the study period. A higher LC value indicates a more intense degree of overall land use transformation

Land Use Transfer Matrix

Typically, land use change has been analyzed using the transfer matrix method across different time periods (Meyer & Früh-Müller, 2020; Chen et al., 2021). The utilization of transfer matrices enables a more profound exploration of the trends and patterns in land use change, thereby providing a scientific foundation for effective land resource management and planning strategies (Luo, 2024; Li et al., 2016).

By conducting spatial overlay analysis on the land use change datasets for the years 2000, 2010, and 2020 in the YRB, and applying spatial statistical methods for further analysis, comprehensive land use transition matrices can be constructed for the periods of 2000–2010 and 2010–2020 in the YRB. This widely adopted approach facilitates a meticulous examination of quantitative structural characteristics while ensuring precision (Mauya et al., 2019; Ma et al., 2024).

The equations are as follows here and below:

$$S_{ij} = \begin{vmatrix} S_{11} & S_{12} & \cdots & S_{1n} \\ S_{21} & S_{22} & \cdots & S_{2n} \\ \cdots & \cdots & \cdots & \cdots \\ S_{n1} & S_{n2} & \cdots & S_{nn} \end{vmatrix} \quad (3)$$

where S represents the land area; n denotes the number of different land use types before and after the transition; i , j (i, j =1,2...n) correspond to the land use types prior to and following the transition, respectively; and S_{ij} signifies the area converted from land use type i to land use type j.

The InVEST Model

The InVEST model (Integrated Valuation of Ecosystem Services and Trade-offs), developed by Stanford University, is a widely utilized tool for estimating carbon stock (Imran & Din, 2021; Piyathilake et al., 2022). Both domestic and international researchers have extensively employed the carbon storage & sequestration module of the InVEST model to assess carbon stocks in various ecosystems (Imran & Din, 2021; Piyathilake et al., 2022). The carbon storage module of the InVEST model categorizes ecosystem carbon storage into four primary pools: aboveground biomass, belowground biomass, soil organic carbon, and dead organic matter. These pools represent the carbon content in all living plants above ground, the carbon stored in plant root systems, the organic carbon present in the soil, and the carbon contained in litter and deceased organic matter respectively (Sione et al., 2023)

The calculations are as follows:

$$C_i = C_{i-above} + C_{i-below} + C_{i-dead} + C_{i-soil} \quad (4)$$

$$C_{total} = \sum_{i=1}^{n} C_i \times S_i \quad (5)$$

In this study, i represents the i-th land use type, with $C_{i\text{-}above}$ indicating the carbon density associated with this land use type. Specifically, $C_{i\text{-}above}$, $C_{i\text{-}below}$, $C_{i\text{-}soil}$, $C_{i\text{-}dead}$ refers to the carbon densities of aboveground biomass, belowground biomass, soil organic matter, and dead organic matter, respectively, for the i-th land use type. The total carbon stock for the region is denoted by C_{total}, while S_i represents the total area of the i-th land use type. Finally, n refers to the total number of land use types considered in the analysis.

Carbon Density and Its Correction

Given that the carbon density data utilized in this study are not based on direct measurements and considering the substantial regional variations of carbon density under diverse climatic conditions, it is imperative to calibrate the nationwide and regional data acquired. According to Raich & Nadelhoffer (1989), the carbon density of biomass and soil organic matter exhibits a significant correlation with mean annual precipitation, while demonstrating a weak association with mean annual temperature. Consequently, this study adjusts the carbon density by referencing the methodologies proposed by Alma et al. (2013) and Giardian & Ryan (2000).

It is calculated as follow:

$$C_{SP} = 3.3968\ MAP + 3996.1\ (R^2 = 0.11) \quad (6)$$

$$C_{BP} = 6.798 \times e^{0.0054 \times MAP} \quad (7)$$

$$C_{BT} = 28 \times MAT + 398 \quad (8)$$

where C_{SP} represents the soil carbon density (kg.m^{-2}) derived from mean annual precipitation; C_{BP} and C_{BT} denote the biomass carbon densities (kg.m^{-2}) obtained based on mean annual precipitation and mean annual temperature, respectively. MAP is the mean annual precipitation (mm); and MAT is the mean annual temperature (°C).

The coefficient was conducted using the following calculations:

$$K_{BP} = \frac{C'_{BP}}{C''_{BP}} \quad (9)$$

$$K_{BT} = \frac{C'_{BT}}{C''_{BT}} \quad (10)$$

$$K_{B} = K_{BT} \times K_{BP} \quad (11)$$

$$K_{S} = \frac{C'_{SP}}{C''_{SP}} \quad (12)$$

where K_{BP} and K_{BT} are the correction coefficients for the precipitation factor and temperature factor of biomass carbon density, respectively; K_B represents the final correction coefficient for biomass carbon density; and K_S is the final correction coefficient for soil carbon density. The product of these correction coefficients and the national carbon density yields the carbon density data for the YRB. The corrected carbon density data are presented in Table 3.1.

Table 3.1: Corrected Carbon Density Data for the Yellow River Basin (Mg C/hm^2)

Land Use Type\Carbon Pools	Aboveground Carbon Density	Belowground Carbon Density	Soil Carbon Density	Dead Organic Matter Carbon Density
Cropland	2.50	0.38	89.24	0.95
Forest	41.93	10.44	102.87	1.80
Grassland	0.40	4.14	82.80	0.08
Water Bodies	0.28	0.97	16.64	1.17
Built-up Land	1.81	4.51	68.22	0.26
Unused Land	1.22	1.95	20.94	0.91

Source from: Xu et al.,2023

Results

Spatiotemporal Characteristics of Land Use Changes in the Yellow River Basin from 2000 to 2020

Spatial Distribution Characteristics of Land Use

From the perspective of land use structure, grassland constitutes the predominant land use type in the YRB, encompassing approximately 47% of the total study area. It is followed by cropland, which accounts for about 31%. As presented in Figure 4.1. The proportions of remaining land use types, including forest, water bodies, built-up land, and unused land, are relatively smaller. Between 2000 and 2020, the area of built-up land witnessed a 2.69% increase, while the areas of unused land and water bodies experienced declines of 2.66% and 0.04%, respectively. In contrast, the areas of cropland, forest, and grassland remained largely unchanged during this period.

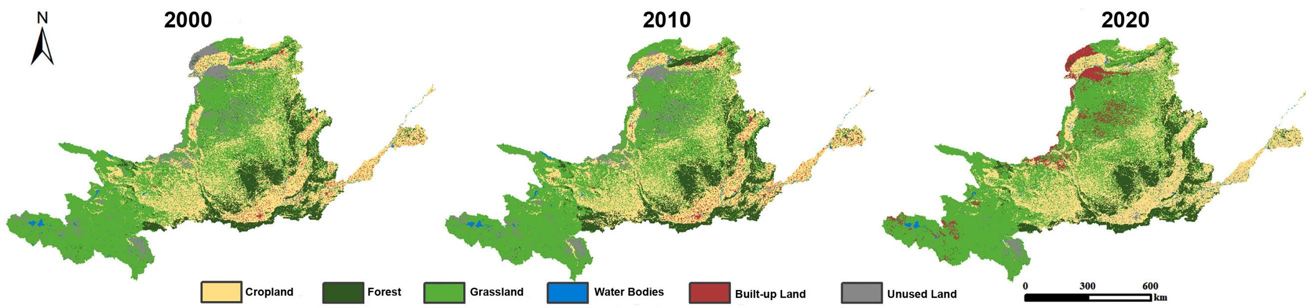

Figure 4.1: Spatial Distribution Map of Land Use in the Yellow River Basin from 2000 to 2020

The extent of land-use change varied markedly among land-use categories over the 20-year study period. The areas of cropland, forest, and grassland exhibited minimal fluctuations, while built-up land and unused land experienced more pronounced alterations. The areas of cropland, forest, and grassland exhibited minimal fluctuations, while built-up land and unused land experienced more pronounced changes. Specifically, the area of built-up land saw significant growth of 151.79%, increasing by 22,247.07 km². In contrast, the area of unused land demonstrated a steady decline with a moderate decrease between 2000 and 2010 followed by a sharp reduction of 44.85% from 2010 to 2020. As demonstrated in Table 4.1.

Table 4.1: Area and Proportion of Different Land Use Types in the Yellow River Basin from 2000 to 2020

Class	2000		2010		2020	
	Area/km²	Proportion/%	Area/km²	Proportion/%	Area/km²	Proportion/%
Cropland	260176.878	31.44%	256147.75	30.96%	260177.85	31.44%
Forest	101046.19	12.21%	112528.01	13.60%	101044.40	12.21%
Grassland	401024	48.47%	392963.55	47.49%	401024.21	48.47%
Water Bodies	6029.33	0.73%	7005.52	0.85%	5743.10	0.69%
Built-up Land	14656.37	1.77%	17912.84	2.16%	36903.45	4.46%
Unused Land	44507.50	5.38%	40882.76	4.94%	22547.17	2.72%

Land Use Dynamics Analysis

From the perspective of individual land use dynamics during 2000 to 2010, the YRB's land use dynamics, ranked by absolute change magnitude, were: built-up land, water bodies, forest, unused land, grassland, and cropland. Built-up land, water bodies, and forest experienced positive values, indicating substantial and rapid increases in their areas during this period. In contrast, the remaining land use types showed negative values, with unused land experiencing the most significant decrease in area. Between 2010 and 2020, except for unused land, all other land use types underwent changes in the opposite direction compared to the previous period, and these changes were more pronounced. The land use types with positive dynamic values - cropland, grassland, and built-up land—experienced increases in area, with built-up land showing the most significant growth, expanding 4.77 times more than in the previous period. The areas of forest, water bodies, and unused land exhibited contrasting trends, with reductions observed in all three categories. Notably, unused land experienced the most substantial decrease in area. Its dynamic value recorded a negative change of -4.48%, indicating a 5.53-fold increase compared to the previous period. The comprehensive land use dynamic indices for the periods 2000-2010 and 2010-2020 were 0.42% and 0.67%, respectively. Notably, the period from 2010 to 2020 experienced a significant increase in the area undergoing land use type transitions, approximately 1.6 times greater than in the previous period. As illustrated in Table 4.2.

Table 4.2: Dynamics of Single and Comprehensive Land Use in the Yellow River Basin from 2000 to 2020

Class	Single land use dynamics/%	
	2000-2010	2010-2020
Cropland	-0.15	0.16
Forest	1.14	-1.02
Grassland	-0.20	0.21
Water Bodies	1.62	-1.80
Built-up Land	2.22	10.60
Unused Land	-0.81	-4.48
Comprehensive land use dynamics/%	0.42	0.67

Land Use Transition Analysis

Between 2000 and 2020, the total land-use transfer area in the YRB reached 827,406.70 km². During this period, grassland and cropland experienced the most significant changes. A detailed analysis of land-use transfer characteristics from 2000 to 2010 indicates that cropland was predominantly converted into grassland and built-up land, followed by forest and water bodies, with only a small proportion transitioning to unused land. Forest, on the other hand, was primarily converted to grassland, followed by cropland, with minor transitions to built-up land, water bodies, and unused land. As shown in Table 4.3.

Table 4.3: Land Use Transition Matrix of the Yellow River Basin from 2000 to 2010 (km²)

2000\2010	Cropland	Forest	Grassland	Water Bodies	Built-up Land	Unused Land	Total/ km²
Cropland	243281.64	2654.12	7567.38	1095.51	5199.13	371.42	260169.19
Forest	1966.34	92342.48	6542.91	38.10	42.78	104.23	101036.84
Grassland	7268.42	17265.57	370771.66	929.38	545.31	4229.11	401009.46
Water Bodies	788.17	71.21	411.51	4420.05	24.66	312.98	6028.57
Built-up Land	2351.66	51.71	171.56	12.30	12059.63	9.11	14655.96
Unused Land	485.54	137.55	7481.90	509.41	40.72	35851.55	44506.66
Total/ km²	256141.77	112522.64	392946.91	7004.75	17912.22	40878.41	827406.70

In the subsequent phase from 2010 to 2020, grassland demonstrated the largest area of change, with 260,169.19 km² transferred, primarily into cropland, forest, and built-up land. Similarly, cropland underwent substantial transitions, with an equivalent area of 260,169.19 km² being converted, predominantly to grassland, unused land, and forest. These findings highlight the dynamic nature of land-use changes within the basin, driven by a complex interplay of ecological, agricultural, and urbanization processes, each contributing to the evolving landscape and carbon dynamics of the region. As present in Table 4.4.

Table 4.4: Land Use Transition Matrix of the Yellow River Basin from 2010 to 2020 (km²)

2010\2020	Cropland	Forest	Grassland	Water Bodies	Built-up Land	Unused Land	Total/ km²
Cropland	243281.64	1966.34	7268.42	788.17	42.92	2794.28	256141.77
Forest	2654.12	92342.48	17265.57	71.06	82.77	106.63	112522.64
Grassland	7567.38	6542.91	370771.66	402.37	6695.38	967.22	392946.91
Water Bodies	1095.51	38.10	929.38	4146.66	128.14	666.96	7004.75
Built-up Land	5199.13	42.78	545.31	24.66	28.95	12071.39	17912.22
Unused Land	371.42	104.23	4229.11	309.74	29924.04	5939.87	40878.41
Total	260169.19	101036.84	401009.46	5742.65	36902.21	22546.35	827406.70

Spatiotemporal Characteristics of Carbon Stock Changes in the Yellow River Basin from 2000 to 2020

The total carbon stock in the YRB was estimated at 7,746.53 × 10^6 t in 2000, 7,836.02 × 10^6 t in 2010, and 7,857.43 × 10^6 t in 2020. Over the two decades, carbon stock exhibited a net increase, with a more pronounced growth of 89.49 × 10^6 t during the 2000–2010 period and a comparatively smaller increment of 21.41 × 10^6 t between 2010 and 2020. As illustrated in Figure 4.2. Grassland, cropland, and forest ecosystems were identified as the predominant contributors to carbon stock within the basin, serving as essential carbon sinks. These ecosystems play a pivotal role in regional carbon sequestration, highlighting their importance in mitigating carbon emissions and sustaining ecological balance within the YRB.

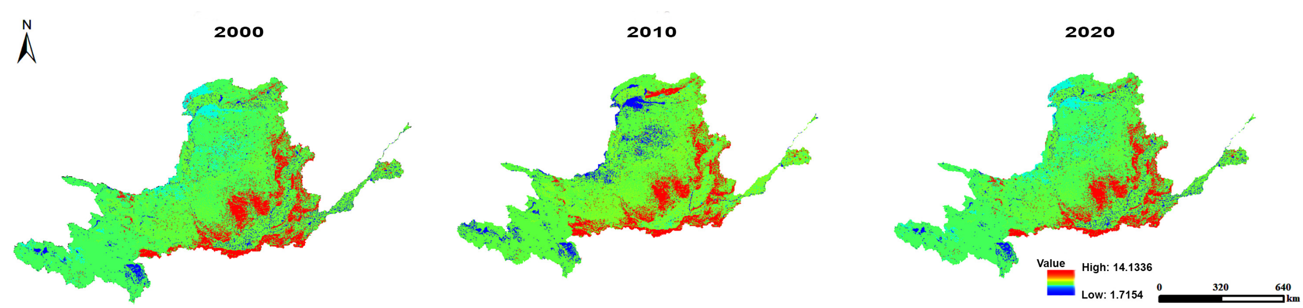

Figure 4.2: Carbon Stock Distribution Map of Yellow River Basin from 2000 to 2020

The Impact of Land Use Changes on Carbon Stock

The changes in carbon stock induced by land-use transformations in the YRB from 2000 to 2020 are presented in Table 4.5. These variations were significantly influenced by the extent of land transitions between different land use types and the disparities in carbon density associated with soil and vegetation. As a result, the impact of such conversions on carbon stock exhibited considerable heterogeneity within land use categories. Over the two decades, the aggregate areas of cropland, grassland, and forest remained relatively stable, thereby contributing minimally to variations in carbon stock. The area of water bodies experienced a slight decline, from 6,029.33 km² to 5,743.10 km²; however, the associated total carbon stock remained constant, indicating the limited impact of this land use category on overall carbon dynamics.

In contrast, the most significant changes in carbon stock were primarily attributed to substantial modifications in the extents of urbanized and unused land. The expansion of built-up land by 22,247.08 km² led to a notable increase in carbon stock, amounting to 183.71 × 10^6 t, underscoring the significant contribution of urbanization to regional carbon dynamics. Conversely, the dramatic contraction of unused land, with its area decreasing by 21,960.33 km², resulted in a comparatively modest reduction in carbon stock, amounting to only 72.79 × 10^6 t.

This discrepancy reflects the inherently low carbon density of unused land, which mitigates its potential impact on regional carbon stocks when subjected to land-use transitions.

Table 4.5: Carbon Stock of Yellow River Basin from 2000 to 2020

Class	2000		2010		2020	
	Area/km^2	Carbon Stock/10^{6}t	Area/km^2	Carbon Stock/10^{6}t	Area/km^2	Carbon Stock/10^{6}t
Cropland	260176.878	2421.45	256147.75	2383.97	260177.85	2421.48
Forest	101046.19	1586.78	112528.01	1767.14	101044.40	1586.80
Grassland	401024	3505.70	392963.55	3435.29	401024.21	3505.75
Water Bodies	6029.33	10.95	7005.52	13.35	5743.10	10.95
Built-up Land	14656.37	92.33	17912.84	133.99	36903.45	276.04
Unused Land	44507.50	129.20	40882.76	102.29	22547.17	56.41

Between 2000 and 2020, variations in carbon stock across the YRB were primarily driven by transitions among cropland, forest, and grassland, even though the overall extent of these land-use types remained relatively stable. As detailed in Table 4.6.

During 2000–2010, grassland-to-forest conversion covered 17,265.57 km² and generated a carbon gain of 120.19 × 10^6t, making it the dominant contributor to carbon sequestration. The conversion of unused land into grassland (7,481.90 km²) added another 46.69 × 10^6 t. In contrast, forest-to-grassland transition (6,542.91 km²) reduced carbon stocks by 45.55 × 10^6 t, partially offsetting these gains. Cropland outflows caused a further net loss of 7.44 × 10^6 t, while the expansion of built-up land contributed an additional 4.82 × 10^6 t.

In the following decade (2010–2020), transition dynamics shifted substantially. Forest-to-grassland conversion expanded to 17,265.57 km², producing a loss of 120.19 × 10^6 t. Total carbon loss from forest outflows reached 140.24 × 10^6 t—79.85 × 10^6 t higher than in the earlier decade. By contrast, grassland-to-forest conversion contributed only 45.55 × 10^6t, a sharp decline from the previous period. Large-scale transformation of unused land into built-up land (29,924.04 km²) added 148.98 × 10^6 t, whereas the reverse pathway—built-up to unused land (12,071.39 km²) has led to a loss of 60.10 × 10^6 t. Cropland outflows also intensified, causing a loss of 16.45 × 10^6 t, more than double that of 2000–2010.

Overall, carbon stock changes in the YRB were largely shaped by transitions between major land-use categories. Conversions such as grassland to forest and unused land to grassland generally enhanced carbon stock, whereas shifts including forest to grassland, unused land to built-up areas, and cropland losses tended to reduce it. These results indicate that the dynamics of carbon stock are governed less by the net expansion or contraction of individual land types than by the specific directions of conversion and the associated differences in carbon density. Among these, the bidirectional exchanges between forest and grassland, together with the transformation of unused land into developed areas, represent the most critical processes driving regional carbon stock change. These findings are broadly consistent with the conclusions of Li et al. (2025), although some differences remain in the specific quantitative outcomes.

Table 4.6: Comprehensive Comparison of Land Use Transitions and Carbon Stock Changes (2000-2010 vs. 2010-2020)

Initial Land Use Type	Converted to -> Final Land Use Type	2000-2010		2010-2020	
		Transferred Area (km²)	Carbon Stock Change (10^6 t)	Transferred Area (km²)	Carbon Stock Change (10^6 t)
Cropland	Forest	2654.12	+16.98	1,966.34	+12.58
	Grassland	7,567.38	-4.28	7,268.42	-4.11
	Water Bodies	1,095.51	-8.11	788.17	-5.83
	Built-up Land	5,199.13	-9.5	42.92	-0.08
	Unused Land	371.42	-2.53	2,794.28	-19.01
	Net Change from Cropland Outflows	16,887.56	-7.44	12,860.13	-16.45
Forest	Cropland	1,966.34	-12.58	2,654.12	-16.98
	Grassland	6,542.91	-45.55	17,265.57	-120.19
	Water Bodies	38.1	-0.53	71.06	-0.98
	Built-up Land	42.78	-0.35	82.77	-0.68
	Unused Land	104.23	-1.38	106.63	-1.41
	Net Change from Forest Outflows	8,694.36	-60.39	20,180.15	-140.24
Grassland	Cropland	7,268.42	+4.11	7,567.38	+4.28
	Forest	17,265.57	+120.19	6,542.91	+45.55
	Water Bodies	929.38	-6.35	402.37	-2.75
	Built-up Land	545.31	-0.69	6,695.38	-8.45
	Unused Land	4,229.11	-26.39	967.22	-6.03
	Net Change from Grassland Outflows	30,237.79	+90.87	22,175.26	+32.60
Water Bodies	Cropland	788.17	+5.83	1,095.51	+8.11
	Forest	71.21	+0.98	38.1	+0.53
	Grassland	411.51	+2.81	929.38	+6.35
	Built-up Land	24.66	+0.14	128.14	+0.71
	Unused Land	312.98	+0.21	666.96	+0.40
	Net Change from Water Bodies Outflows	1,608.53	+9.97	2,858.09	+16.10
Built-up Land	Cropland	2,351.66	+4.29	5,199.13	+9.49
	Forest	51.71	+0.42	42.78	+0.35
	Grassland	171.56	+0.22	545.31	+0.69
	Water Bodies	12.3	-0.07	24.66	-0.14
	Unused Land	9.11	-0.04	12,071.39	-60.1
	Net Change from Built-up Land Outflows	2,596.34	+4.82	17,883.27	-49.71
Unused Land	Cropland	485.54	+3.30	371.42	+2.53
	Forest	137.55	+1.82	104.23	+1.38
	Grassland	7,481.90	+46.69	4,229.11	+26.39
	Water Bodies	509.41	-0.3	309.74	-0.18
	Built-up Land	40.72	+0.20	29,924.04	+148.98
	Net Change from Unused Land Outflows	8,655.12	+51.71	34,938.54	+179.10

Conclusion

Building upon two decades of land use data and utilizing the InVEST model, this study conducts a comprehensive spatiotemporal analysis of the dynamics in land use patterns and changes in carbon stock within the YRB. Furthermore, it investigates the implications of land use transformations on the region's carbon stock.

The findings reveal that between 2000 and 2020, the land use structure of the YRB underwent significant transformations. While there were relatively minor changes in the total areas of cropland, grassland, forest, and water bodies, substantial shifts were observed in the areas of built-up land and unused land. Specifically, the area of built-up land expanded dramatically by 22,247.07 km², reflecting a remarkable growth rate of 151.79%. The converse trend was observed in the case of unused land, which underwent a substantial decrease with its area contracting by 21,960.33 km² over the course of two decades, corresponding to a reduction of 49.34%. Despite some fluctuations, the carbon stock in the YRB remained relatively stable between approximately 7,746.53 × 10^6 t and 7,857.43 × 10^6 t from 2000 to 2020, even with the implementation of ecological restoration projects such as the Grain for Green Program. The impact of land use transitions on carbon stock varies significantly among different land use types. Transitions involving cropland, grassland, and forest exert a relatively substantial influence on carbon stock. The ultimate impact of these transitions, however, is moderated by the implementation of ecological restoration initiatives, thereby constraining their overall effect on carbon stock. Conversely, despite the inherently low carbon densities of built-up land and unused land, their pronounced changes in area have had a significant cumulative impact on carbon stock dynamics.

Although this study improves our understanding of how land use change influenced carbon stocks in the YRB between 2000 and 2020, it is not without limitations. A major concern is that the carbon density parameters were mostly drawn from previous studies. While widely used, these values may not fully represent the spatial differences within each land-use type or their changes over time, which could lead to some bias in the estimates. Another limitation is related to the modeling framework: the InVEST model, together with the GlobeLand30 dataset, captures patterns of land use and carbon stock well, but it does not take into account certain natural processes such as climate variation, soil characteristics, or vegetation succession. These processes might play a stronger role than we have captured here. Finally, this study has mainly concentrated on historical transitions. This study did not extend the analysis to simulate future land use under alternative scenarios, nor did it test how different policy measures could affect long-term carbon dynamics.

These limitations highlight promising directions for future research. For example, more precise and locally calibrated carbon density values could be developed from field surveys and remote sensing. Different models could be compared to better identify the mechanisms driving land use–carbon relationships. It would also be valuable to include scenario analysis, especially under contrasting policies such as afforestation versus urban expansion, and to link carbon stock with other ecosystem services.

Research contribution

This study systematically examines land use changes and their impacts on carbon stocks in the YRB, highlighting how dynamic transitions among land use types shape both carbon accumulation and release. By comparing the complex land use transfers and the associated carbon stock variations across two time periods, the findings not only provide new empirical evidence on the land use–carbon stock relationship but also enrich the process-oriented understanding of carbon sequestration mechanisms. These insights suggest that guiding land use transitions appropriately can strengthen regional carbon sinks and offer scientific support for achieving national Carbon Neutrality goals.

Methodologically, this study integrates land use dynamic indices and transition matrices with the InVEST model to establish a multidimensional analytical framework. This approach enables not only the quantification of land use conversion pathways and their magnitudes across different periods but also the explicit identification of the carbon stock effects associated with each transition. Such a framework offers a refined and systematic pathway for analyzing land use dynamics and their carbon implications.

Practical contributions

This study holds significant practical implications, particularly for land use and carbon management policies in the YRB. Firstly, it provides a scientifically grounded foundation for land use planning in the region, aiding governmental efforts to optimize land use structures and enhance carbon stock. By conducting a quantitative analysis of the impact of various land use types on carbon stock, this study can provide robust data support for informed land use decision-making and facilitate the advancement of a low-carbon economy. Additionally, it aids local governments in formulating effective policies for managing carbon emissions, particularly through the establishment of carbon sinks and implementation of ecological restoration measures.

Acknowledgement

We appreciate the financial support of this study from Carbon Sink Efficiency and Incremental Optimization of Green Spaces in High-Density Urban Areas of Chongqing: A Study Towards Carbon Neutrality (Project Number: KJQN202302502).

References

Alam, S. A., Starr, M., & Clark, B. J. F. (2013). Tree Biomass and Soil Organic Carbon Densities Across the Sudanese Woodland Savannah: A Regional Carbon Sequestration Study. *Journal of Arid Environments*, *89*, 67-76. https://doi.org/10.1016/j.jaridenv.2012.10.002

Chen, H. X., Chen, C., Zhang, Z. L., Lu, C., Wang, L. Y., He, X. Y., Chu, Y. L., & Chen, J. Y. (2021). Changes of the Spatial and Temporal Characteristics of Land-Use Landscape Patterns Using Multi-Temporal Landsat Satellite Data: A Case Study of Zhoushan Island, China. *Ocean & Coastal Management*, *213*, 105842. https://doi.org/10.1016/j.ocecoaman.2021.105842

Giardina, C. P., & Ryan, M. G. (2000). Evidence that Decomposition Rates of Organic Carbon in Mineral Soil do not Vary with Temperature. *Nature*, *404*(6780), 858–861. https://doi.org/10.1038/35009076

Huang, G. X., & Wang, R. Y. (2023). Impact of Land Use/Cover Change (LUCC) on Carbon Storage in Zhaoqing by using the InVEST Model. International Journal of Rural Development, *Environment and Health Research*, *7*(4), 20–37. https://doi.org/10.22161/ijreh.7.4.2

Imran, M., & Din, N. (2021). Geospatially Mapping Carbon Stock for Mountainous Forest Classes Using Invest Model and Sentinel-2 Data: A Case of Bagrote Valley in the Karakoram Range. *Arabian Journal of Geosciences*, *14*(9), 756. https://doi.org/10.1007/s12517-021-07023-4

Jian, S. Q., Zhang, Q. K., & Wang, H. L. (2022). Spatial–Temporal Trends in and Attribution Analysis of Vegetation Change in the Yellow River Basin, China. *Remote Sensing*, *14*(18), 4607. https://doi.org/10.3390/rs14184607

Li, J., Bai, L. Y., Li, J. R., Nie, Y. H., Yang, P. G., Qin, J. H., & Qu, R. (2016). Monitoring and Analysis of Land Use Change in Xiamen Harbor Area Based on Multi-Source Remote Sensing Images. *2016 IEEE International Geoscience and Remote Sensing Symposium (IGARSS)*, 7303–7306. https://doi.org/10.1109/IGARSS.2016.7730905

Li, J. Y., Gong, J., Guldmann, J. M., Li, S. C., & Zhu, J. (2020). Carbon Dynamics in the Northeastern Qinghai–Tibetan Plateau from 1990 to 2030 Using Landsat Land Use/Cover Change Data. *Remote Sensing*, *12*(3), 528. https://doi.org/10.3390/rs12030528

Li, K. Y., Wang, X. M., Zhao, F., & An, B. S. (2024). Land Use Modeling and Carbon Storage Projections of the Bosten Lake Basin in China from 1990 to 2050 Across Multiple Scenarios. *Scientific Reports, 14*, 27136. https://doi.org/10.1038/s41598-024-78693-9

Li, M., Wu, D. L., He, H., Yu, H. J., Zhao, L., Liu, C., Hu, Z. H., & Li, Q. (2025). Spatio-Temporal Evolution and Driving Factors of Carbon Storage in the Yellow River Basin from 1990 to 2020. *Ecology and Environmental Sciences, 34*(3), 333–344.

Li, Y. Q., Li, J. R., Jiao, S. Y., Li, Y., Xu, Z. Y., & Kong, B. S. (2020). Ecosystem-Scale Carbon Allocation Among Different Land Uses: Implications for Carbon Stocks in the Yellow River Delta. *Ecosphere, 11*(5), e03125. https://doi.org/10.1002/ecs2.3125

Luo, H. (2024). Evaluation of Land Use and Land Cover Change and Spatial Ecological Impacts Using GIS: A Case Study of Urumqi's Primary Urban Area. *Highlights in Business, Economics and Management, 26*, 138–144. https://doi.org/10.54097/1qd0sj72

Ma, W. J., Hou, S. J., Su, W. F., Mao, T., Wang, X. Y., & Liang, T. T. (2024). Estimation of Carbon Stock and Economic Value of Sanjiangyuan National Park, China. *Ecological Indicators, 169,* 112856. https://doi.org/10.1016/j.ecolind.2024.112856

Ma, R. H. (2024, November 15). *Yellow River Basin Township Administrative Boundary Dataset*. National Earth System Science Data Center. http://www.geodata.cn/

Malik, A. D., Arief, M. C. W., Withaningsih, S., & Parikesit, P. (2023). Modeling Regional Aboveground Carbon Stock Dynamics Affected by Land Use and Land Cover Changes. *Global Journal of Environmental Science and Management, 10*(1), 245-266. https://doi.org/10.22034/gjesm.2024.01.16

Mauya, E. W., Mugasha, W. A., Njana, M. A., Zahabu, E., & Malimbwi, R. (2019). Carbon Stocks for Different Land Cover Types in Mainland Tanzania. *Carbon Balance and Management, 14*(1), 4. https://doi.org/10.1186/s13021-019-0120-1

Meyer, M. A., & Früh-Müller, A. (2020). Patterns and Drivers of Recent Agricultural Land-Use Change in Southern Germany. *Land Use Policy, 99*, 104959. https://doi.org/10.1016/j.landusepol.2020.104959

National Geomatics Center of China. (2024, November 15). *Globeland 30 Dateset*. National Catalogue Service For Geographic Information. https://www.webmap.cn/commres.do?method=globeIndex

Peng, S. Z., Ding, Y. X., Liu, W. Z., & Li, Z. (2024, November 20). *1 KM Monthly Temperature and Precipitation Dataset for China from 1901 to 2017*. Earth System Science Data. https://www.geodata.cn/data/datadetails.html?dataguid=164304785536614&docId=490

Piyathilake, I. D. U. H., Udayakumara, E. P. N., Ranaweera, L. V., & Gunatilake, S. K. (2022). Modeling Predictive Assessment of Carbon Storage Using Invest Model in Uva Province, Sri Lanka. *Modeling Earth Systems and Environment, 8*(2), 2213–2223. https://doi.org/10.1007/s40808-021-01207-3

Sione, S. M. J., Wilson, M. G., Ledesma, S. G., Gabioud, E. A., Oszust, J. D., & Rosenberger, L. J. (2023). Driving Factors of Tree Biomass and Soil Carbon Pool in Xerophytic Forests of Northeastern Argentina. *Ecological Processes, 12*(1), 64. https://doi.org/10.1186/s13717-023-00478-1

Sun, B.Q., Du,J.Q., Chong, F.F., & Li, L.J. (2023). Spatio-Temporal Variation and Prediction of Carbon Storage in Terrestrial Ecosystems in the Yellow River Basin. *Remote Sensing, 15*(15),3866. https://doi.org/10.3390/rs15153866

Wang, J. F., Li, L. F., Li, Q., Wang, S., Liu, X. L., & Li, Y. (2022). The Spatiotemporal Evolution and Prediction of Carbon Storage in the Yellow River Basin Based on the Major Function-Oriented Zone Planning. *Sustainability, 14*(13), 7963. https://doi.org/10.3390/su14137963

Xu, C. L., Zhang, Q. B., Yu, Q., Wang, J. P., Wang, F., Qiu, S., Ai, M. S., & Zhao, J. K. (2023). Effects of Land Use/Cover Change on Carbon Storage Between 2000 and 2040 in the Yellow River Basin, China. *Ecological Indicators, 151*, 110345. https://doi.org/10.1016/j.ecolind.2023.110345

Xu, L., He, N. P., & Yu, G. R. (2024, November 21). *2010s Carbon Density Dataset of Terrestrial Ecosystems in China*. National Data Center for Eco-Science. https://doi.org/10.11922/sciencedb.603

Yang, J. Xie, B.P., & Zhang, D.G. (2021). Spatiotemporal Evolution of Carbon Stocks in the Yellow River Basin Based on Invest and CA-Markov Models. *Chinese Journal of Eco-Agriculture, 29*(6), 1018-1029. https://doi.org/10.13930/j.cnki.cjea.200746

Yang, S., Li, L. Q., Zhu, R. H., Luo, C., Lu, X., Sun, M. L., & Xu, B. C. (2024). Assessing Land-Use Changes and Carbon Storage: A Case Study of the Jialing River Basin, China. *Scientific Reports, 14*(1), 15984. https://doi.org/10.1038/s41598-024-66742-2

Zhao, Z. H., Liu, G. H., & Xu, Z. R. (2018). The Ecosystem Carbon Storage Dataset in Tibet (2001-2010). *Journal of Global Change Data & Discovery, 2*(1), 67–71. https://doi.org/10.3974/geodp.2018.01.11

Zafar, Z., Zubair, M., Zha, Y., Mehmood, M. S., Rehman, A., Fahd, S., & Nadeem, A. A. (2024). Predictive Modeling of Regional Carbon Storage Dynamics in Response to Land Use/Land Cover Changes: An InVEST-based analysis. *Ecological Informatics, 82*, 102701. https://doi.org/10.1016/j.ecoinf.2024.102701

Zeng, Q. Y., Sun, C. Z. (2024). Estimation and Influencing Factors of Carbon Storage in Terrestrial Ecosystems in the Yellow River Basin. *Acta Ecologica Sinica, 44*(13), 5476-5493. http://dx.doi.org/10.20103/j.stxb.202311012367

Zhang, B.,Li, L., Xia, Q.Y., & Dong, J. (2022). Land Use Change and its Impact on Carbon Storage Under the Constraints of “Three Lines”: A Case Study of Wuhan City Circle. *Acta Ecologica Sinica, 42*(6), 2265-2280. https://doi.org/10.5846/stxb202101070075

Zhang, J. J., Yang, J., Liu, P. F., Liu, Y., Zheng, Y. W., Shen, X. Y., Li, B. C., Song, H. Q. , & Liang, Z.Z. (2024). Effects of Land Use/Cover Change on Terrestrial Carbon Stocks in the Yellow River Basin of China from 2000 to 2030. *Remote Sensing, 16*(10), 1810. https://doi.org/10.3390/rs16101810